

INFLUENCE OF VISCOSITY FUNCTION SIMPLIFICATION  
ON NON-NEWTONIAN VELOCITY AND SHEAR-RATE PROFILES  
IN RECTANGULAR DUCTS

M. KOSTIC  
Department of Mechanical Engineering  
NORTHERN ILLINOIS UNIVERSITY  
DeKalb, IL 60115

(Communicated by J.P. Hartnett and W.J. Minkowycz)

**ABSTRACT**

The velocity, shear-rate, variable viscosity, and variable power-law index profiles are calculated for non-Newtonian fluids using the finite difference method. The calculations are carried out for an actual viscosity function obtained by a curve fit through measured data and for the corresponding power law model, the simplest and most often used form for non-Newtonian viscosity function approximation. The obtained results are compared between themselves and with reference results of Newtonian flow. The objective was to determine the influence of an experimental non-Newtonian viscosity function and its simplification on the above profiles. Interestingly, but not surprisingly, the influence of viscosity function simplification is very weak on the velocity profile, somewhat stronger on the shear-rate profile, while the corresponding differences of viscosity and local power-law index profiles are remarkable. Some other characteristic results along with appropriate analysis are presented.

**Introduction**

The analysis of hydrodynamics and heat and mass transfer processes in non-circular duct flows is generally more complex and rarer than in the case of circular pipe flows. Even for the simplest case of laminar and fully developed flow, the velocity profiles are rather complex. Although the partial differential equation of motion for Newtonian fluid flow in a rectangular duct is linear (for fully developed flow the non-linear convective acceleration terms vanish) its solution is not straightforward, but is typically given in terms of an infinite series representation by *Hartnett and Kostic* [1], and *Kostic and Wang* [2]. For more complex, non-Newtonian fluids (where viscosity depends on velocity gradients) the velocity and shear rate profiles have to be obtained by numerical methods owing to the fact that the equation of motion for a non-Newtonian fluid is a non-linear partial differential equation. The usual boundary condition for internal

channel flow of any fluid is the relatively simple no-slip condition, i.e. the velocity goes to zero at the wall boundaries.

It is useful to examine the simple case of velocity profiles for a limiting "zero" aspect ratio, parallel plates channel, in order to show the general influence of the non-Newtonian fluid parameters (namely, the power-law index " $n$ ") on the velocity profile. Another essential influence on the velocity profile in non-Newtonian flow is viscosity dependence on velocity gradients. The power-law fluid model allows for viscosity dependence on shear rate but does not provide for experimentally observed limiting constant values of apparent viscosity for very small and very high shear rates. That is why the velocity profile is obtained numerically for a viscosity function obtained by a curve fit through measured data and compared with a corresponding average power-law fluid model simplification. A variety of results are presented and analyzed for different rectangular duct aspect ratios and different kinds of non-Newtonian fluids.

### Fluids Considered

The velocity and shear-rate profiles and other characteristic flow and fluid properties are obtained and analyzed for the following fluids:

**Newtonian fluids:** At constant temperature (isothermal flow situation), the fluid viscosity does not depend on flow condition, i.e.:

$$\eta = \frac{\tau}{\dot{\gamma}} = \text{constant} \quad (1)$$

**Non-Newtonian power-law model fluids:** The so called apparent viscosity is defined in the same manner as for Newtonian fluids, although it is no longer constant, but depends on flow conditions (shear rate magnitude, for example). For the simplest model of the power-law fluid, the (apparent) viscosity is expressed as:

$$\eta = \frac{\tau}{\dot{\gamma}} = K \dot{\gamma}^{n-1} \quad (2)$$

Here,  $K$  and  $n$  are consistency and power-law indices respectively; both are constant for a given fluid. Note that a special case:  $K=C=\text{constant}$  and  $n=1$ , corresponds to a Newtonian fluid with  $\eta=K=C$ .

**Real (arbitrary) fluid:** In this article the term "*real fluid*" means a fluid with a viscosity function obtained by a curve fit through measured viscosity data. In particular, the measured shear stress data of a 0.1% aqueous polyacrylamide solution as a function of shear rate (FIG.1A), were curve fitted by the following equation:

$$\log \tau = a_0 + a_1(\log \dot{\gamma}) + a_2(\log \dot{\gamma})^2 + a_3(\log \dot{\gamma})^3 \tag{3}$$

where, for the measured shear stress in  $[N/m^2]$  in the shear rate range  $(0.027 s^{-1} \leq \dot{\gamma} \leq 0.55 \cdot 10^5 s^{-1})$ , the coefficients  $a_i = -0.9252, 0.6136, -0.07804, 0.01924$ ; for  $i=0,1,2,3$  respectively. For the measured shear rate range, apparent viscosity and variable power-law index are calculated as:

$$\eta = \eta(\dot{\gamma}) = \frac{\tau}{\dot{\gamma}} = \frac{10^{a_0 + a_1(\log \dot{\gamma}) + a_2(\log \dot{\gamma})^2 + a_3(\log \dot{\gamma})^3}}{\dot{\gamma}} \tag{4}$$

$$n = n(\dot{\gamma}) = \frac{d(\log \tau)}{d(\log \dot{\gamma})} = a_1 + 2a_2(\log \dot{\gamma}) + 3a_3(\log \dot{\gamma})^2$$

both,  $\eta$  and  $n$  being dependent on shear rate. For shear rate  $\dot{\gamma} < 0.027 s^{-1}$ , the viscosity is constant and equal to that of Eq.(4) for  $\dot{\gamma} = 0.027 s^{-1}$  and the power-law index is equal to unity. For shear rate  $\dot{\gamma} > 0.55 \cdot 10^5 s^{-1}$ ,

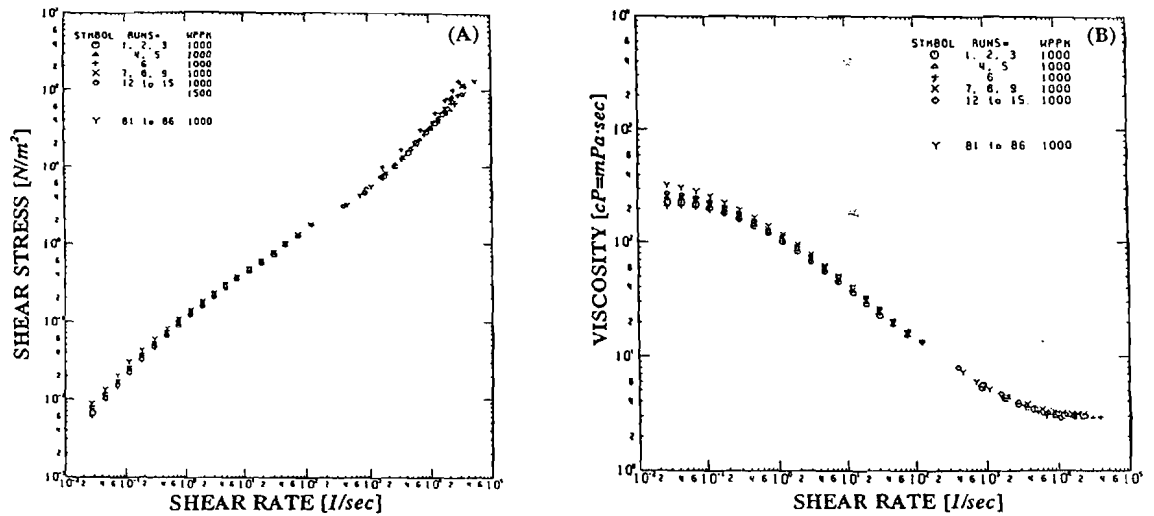


FIG. 1  
Measured Shear Stress (A); and Apparent Viscosity (B), as Function of Shear Rate for 0.1% Polyacrylamide aqueous solution

the viscosity is also constant and equal to that of Eq.(4) for  $\dot{\gamma} = 0.55 \cdot 10^5 s^{-1}$  and the power-law index is again equal to unity (like Newtonian fluid in these limiting shear rate ranges, see FIG.1B).

The reference viscosity used in the generalized Reynolds number, Eq.(7), is determined as an average around the perimeter due to the fact that the friction factor is based on the averaged wall shear stress. Note that for  $a_2 = a_3 = 0$ , the "real fluid" becomes the power-law fluid with the power-law index  $n = a_1$  (if  $a_1 = 1$  then fluid is Newtonian) while  $a_0$  may be arbitrary.

**Average power-law fluid:** This fluid is represented by the power-law model fluid with the power-law index  $n_{ave}$ , obtained by averaging the variable power-law indices of the "real fluid" around the wall perimeter, see the above comment. The "real fluid" results will be compared with this simplified "average

power-law" model in order to see the influence of the viscosity function simplification on the velocity and shear-rate fields.

### Governing Equations

The rectangular duct flow phenomena are reviewed by *Shah and London* [3] for Newtonian fluids, and by *Hartnett and Kostic* [1] for Newtonian and non-Newtonian fluids. For fully developed flow of an incompressible fluid in a rectangular duct geometry (see FIG.2), which is the subject of this article, the continuity equation ( $\nabla \cdot \mathbf{V} = \text{div} \cdot \mathbf{V} = 0$ ) is automatically satisfied, and therefore not needed. However, it is used as a check during the numerical iterative procedure. For fully developed channel flow in  $x$ -direction [ $v=w=0$ ,  $\partial p/\partial y = \partial p/\partial z = 0$  and  $u=u(y,z)$ ,  $\partial p/\partial x = dp/dx = \text{constant}$ ], the momentum equation is also simple:

$$\frac{\partial}{\partial y} \left( \eta \frac{\partial u}{\partial y} \right) + \frac{\partial}{\partial z} \left( \eta \frac{\partial u}{\partial z} \right) + \left( -\frac{dp}{dx} \right) = 0 \quad (5)$$

Here, the (apparent) viscosity  $\eta$  is either constant for constant-temperature Newtonian fluid, or a function of shear rate magnitude (i.e. velocity gradients) as seen in previous section. The corresponding shear rate magnitude  $\dot{\gamma}$  (needed for determination of apparent viscosity), for the case of fully developed flow in rectangular ducts, is expressed by:

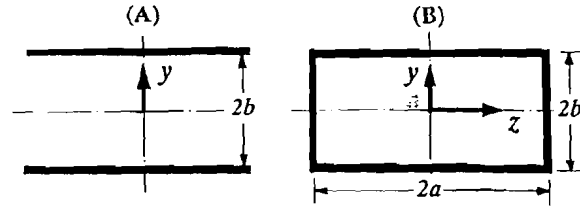


FIG. 2  
Parallel Plates (A), and Rectangular Duct Geometry (B)

$$\dot{\gamma} = \sqrt{\dot{\gamma}_{xy}^2 + \dot{\gamma}_{xz}^2} = \sqrt{(\partial u/\partial y)^2 + (\partial u/\partial z)^2} \quad (6)$$

**Dimensionless quantities:** In order to simplify the governing equations and to facilitate numerical solutions, the physical quantities ( $X_i$ ) are divided by corresponding reference quantities ( $X_{ref,i}$ ) and thereby made dimensionless ( $X_i^* = X_i/X_{ref,i}$ ). The followings reference quantities are used here, if not otherwise stated:

- aspect ratio of rectangular duct:  $\alpha^* = b/a$  (note:  $b \leq a$ ,  $0 \leq \alpha^* \leq 1$ , the limiting values of  $\alpha^* = 0$  and 1 correspond to parallel plates and square ducts respectively, see FIG.2)
- reference length:  $\ell_{ref} = D_h = [4ab]/[(a+b)] = a[4\alpha^*/(1+\alpha^*)] = b[4/(1+\alpha^*)] = \text{hydraulic diameter (FIG.2)}$
- reference velocity:  $u_{ref} = U$ , the cross-sectional-average velocity
- reference shear rate:  $\dot{\gamma}_{ref} = U/D_h$
- reference viscosity:  $\eta_{ref} = \eta_{ave}$  perimeter-average viscosity, or  $\eta_{ref} = K\dot{\gamma}_{ref}^{n-1}$  for power-law fluid
- reference pressure gradient:  $(-dp/dx)_{ref} = \eta_{ref} U/D_h^2$

Taking into account the usual definition of the Fanning friction factor and the generalized Reynolds number

$$f = \frac{\tau_{wall}}{\frac{1}{2}\rho U^2} = \frac{(-\frac{dp}{dx})(\frac{D_h}{4})}{\frac{1}{2}\rho U^2} \quad \text{and} \quad R_e^* = \frac{\rho U D_h}{\eta_{ref}} \quad (7)$$

the dimensionless pressure gradient, usually phrased as "source term" in numerical methods, may be expressed as:

$$\left(-\frac{dp}{dx}\right)^* = \left(-\frac{dp}{dx}\right) / \left(-\frac{dp}{dx}\right)_{ref} = 2fR_e^* \quad (8)$$

For a given fluid and duct aspect ratio the "source term" is constant. Now, the momentum equation, Eq.(5), may be transferred into the following dimensionless form:

$$\frac{\partial}{\partial y^*} \left( \eta^* \frac{\partial u^*}{\partial y^*} \right) + \frac{\partial}{\partial z^*} \left( \eta^* \frac{\partial u^*}{\partial z^*} \right) + 2fR_e^* = 0 \quad (9)$$

Note that the dimensionless viscosity  $\eta^* = 1$  for Newtonian fluids, therefore the above momentum equation becomes linear. Also note that dimensionless volume flow rate (based on dimensionless velocity and per unit of cross-sectional area) is always equal unity, and the boundary condition at the walls is  $u^* = 0$ .

### Numerical Solution Method and Results

For variable viscosities  $\eta$  (or dimensionless  $\eta^*$ ), the momentum equation may only be solved numerically. A finite difference method (in FORTRAN program) is developed, capable of solving for fully developed velocity and shear rate profiles for any fluid with a given viscosity function and for a given aspect ratio rectangular duct (Wang [4]). To increase solution speed the program treats Newtonian and simple power-law non-Newtonian fluids as special cases. The finite difference method suggested by Patankar [5] is adapted here with some modification. The boundary grid point quantities (including corners) are forced to satisfy the boundary conditions. Initial condition (velocity profile guess) is needed and may be arbitrary. However, the program is made more efficient by initializing velocities using available approximate algebraic solution of Newtonian fluids, and even the source term is initially

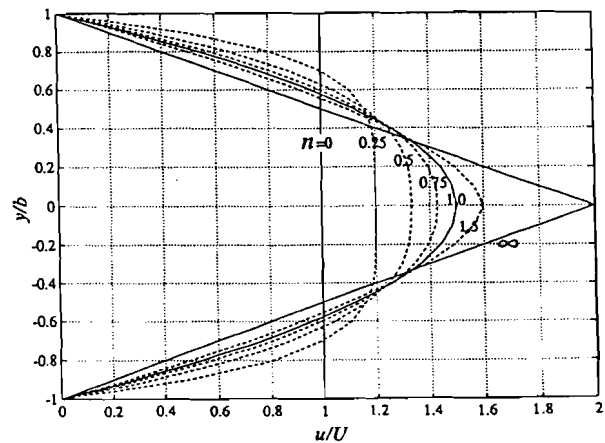


FIG. 3  
Velocity Profiles for Different Power-law Non-Newtonian Fluids in Parallel Plates Duct ( $n=1$  corresponds to Newtonian Fluid)

"guessed" by using available solutions for Newtonian and/or the power-law fluids [1]. The dimensionless momentum equation is solved by using the iterative tri-diagonal-matrix-algorithm (TDMA), sweeping the rows from bottom-to-top wall and back, and then columns from right-to-left wall and back, in order to facilitate symmetricity (and stability) and speed of convergence by bringing the boundary values influence speedily into the interior. Before each iterations is carried out for non-Newtonian fluids, the dimensionless shear rates and viscosities are calculated for all grid points in separate subroutines. Detailed description of the program is given by Wang [4]. Note that the governing equation may be solved analytically for two special cases: namely, Newtonian fluid ( $\eta^*=1$ ) and any aspect ratio duct (in form of infinite series solution); and for the power-law non-Newtonian fluid flow in parallel plates duct ( $n=constant$  and  $\alpha^*=0$ ) [1].

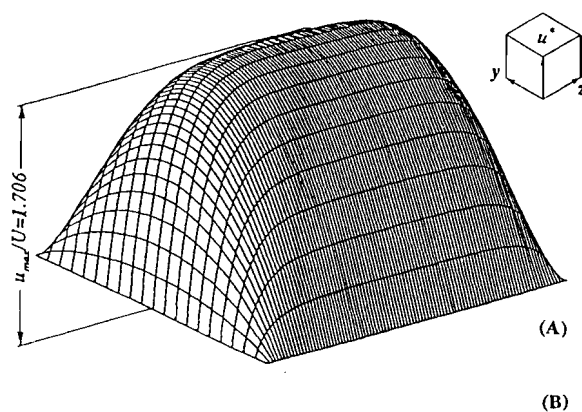
The dimensionless velocity profile (DVP), as the solution of the dimensionless momentum equation, Eq. (9), depends on the duct geometry (i.e. aspect ratio  $\alpha^*$ ) and dimensionless viscosity function  $\eta^*=\eta^*(\dot{\gamma}^*)$ . Note that: for Newtonian fluid  $\eta^*=1$  (the DVP is not dependent on fluid properties); for the power-law non-Newtonian fluid  $\eta^*=\eta^*(n)$ , i.e. the DVP is dependent on power-law index  $n$  only (not on the consistency index  $K$  which cancels out); and for an arbitrary viscosity function  $\eta^*$ , dimensionless velocity profile depends, in addition on the aspect ratio  $\alpha^*$ , also on all the coefficients  $a_i$ 's of the viscosity function (in our case  $i=0,1,2,3$ ).

Summaries of the most characteristic numerical results are given in TABLES 1 to 4. The shaded-area results in the Tables are emphasized for comparison purposes and some are detailed in FIGS.4 to 8. The maximum velocities, which occur at the center-point of the duct cross-section, are given in TABLE 1, for different duct aspect ratios and fluids (different  $n$ 's, including "real" and "average" fluids). It is interesting to note that maximum shear rate values are always at the center of the longer wall, and are given in TABLE 2 for different ducts and fluids. The shear rates are also given for two other characteristic points: the center of the shorter wall (TABLE 3), and at the corners in TABLE 4. Note that velocities at walls and shear rate at the center-point of the duct cross-section are minimum, i.e. equal to zero. Also note that all quantities given are dimensionless if not otherwise stated.

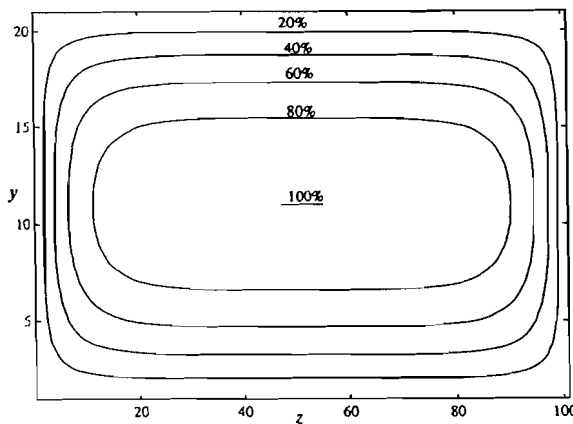
The available analytic (exact) solutions for power-law non-Newtonian fluid flow in a parallel plates duct (FIG.3), and infinite series solutions for Newtonian fluid in a rectangular duct (FIGS.4&5) are presented [2]. The former shows the influence of non-Newtonian fluid properties on the velocity profiles, while the latter represents the reference results against which the numerical method is validated and other results are compared. Then, the calculated numerical results of velocity, shear rate, viscosity, and variable power-law index profiles, for the so called "real" non-Newtonian fluid, are presented on FIGS.6,7&8.

#### Analysis and Conclusion

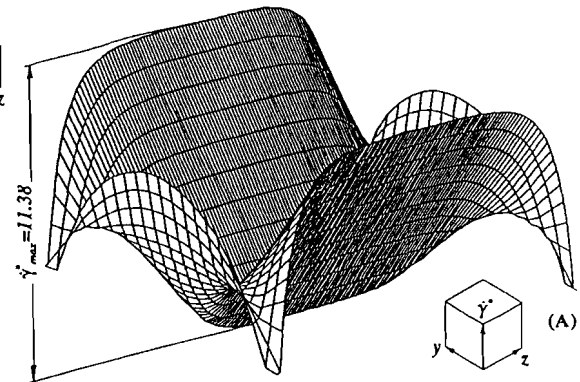
The viscosity dependence on shear rate (through the power-law index  $n$ ) influences the velocity profile, as seen on FIG.3, for the simplest duct geometry ( $\alpha^*=0$ ). The more viscosity decreases with



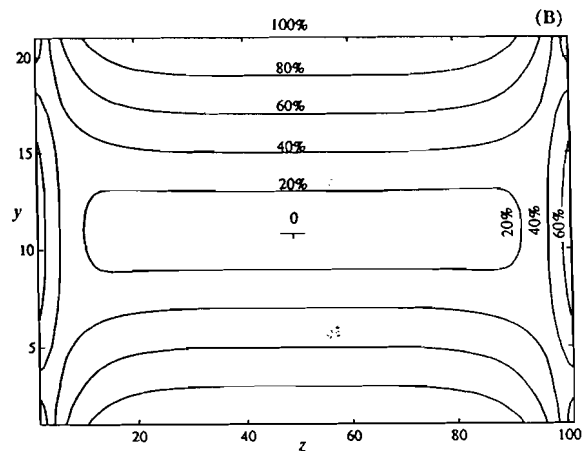
(A)



(B)



(A)



(B)

FIG. 4

(A) Velocity Profile for Newtonian Fluid;  
(B) Corresponding Iso-Velocity Contours

FIG. 5

(A) Shear Rate Profile for Newtonian Fluid;  
(B) Corresponding Iso-Shear-Rate Contours

increase of shear rate (which is represented by decrease of power-law index  $n$  from 1 to 0) the velocity profile becomes flatter, reaching a uniform distribution (slug or plug flow) for the limiting case of  $n=0$ . For the power-law index values  $n \geq 1$ , the phenomena are opposite, and the limiting velocity profile becomes linear for  $n$  approaching infinity.

The velocity profile of a Newtonian fluid in a 1:5 rectangular duct is presented on FIG.4. Maximum velocity at the center-point is 1.715 of the average velocity, higher than for the parallel plates case because of more flow retardation by four walls (as compared to two, for parallel plates). Iso-velocity contours have tendency to accommodate in shape the walls boundary. The shear rate (velocity gradients) distribution, FIG.5, is more complex. The maximum shear rate is always at the center of the longer wall, then it is smaller at near the corner region, and finally, through a saddle-type of surface, shear rate reaches its minimum (zero value) at the center-point of a duct cross-section.

Numerical results of velocity, shear rate, viscosity and variable power-law index profiles, for the so called "real" non-Newtonian fluid are presented on FIGS.6,7&8. These results may be compared with the corresponding results of Newtonian fluid on FIGS.4&5. The "real" non-Newtonian velocity profile of FIG.6

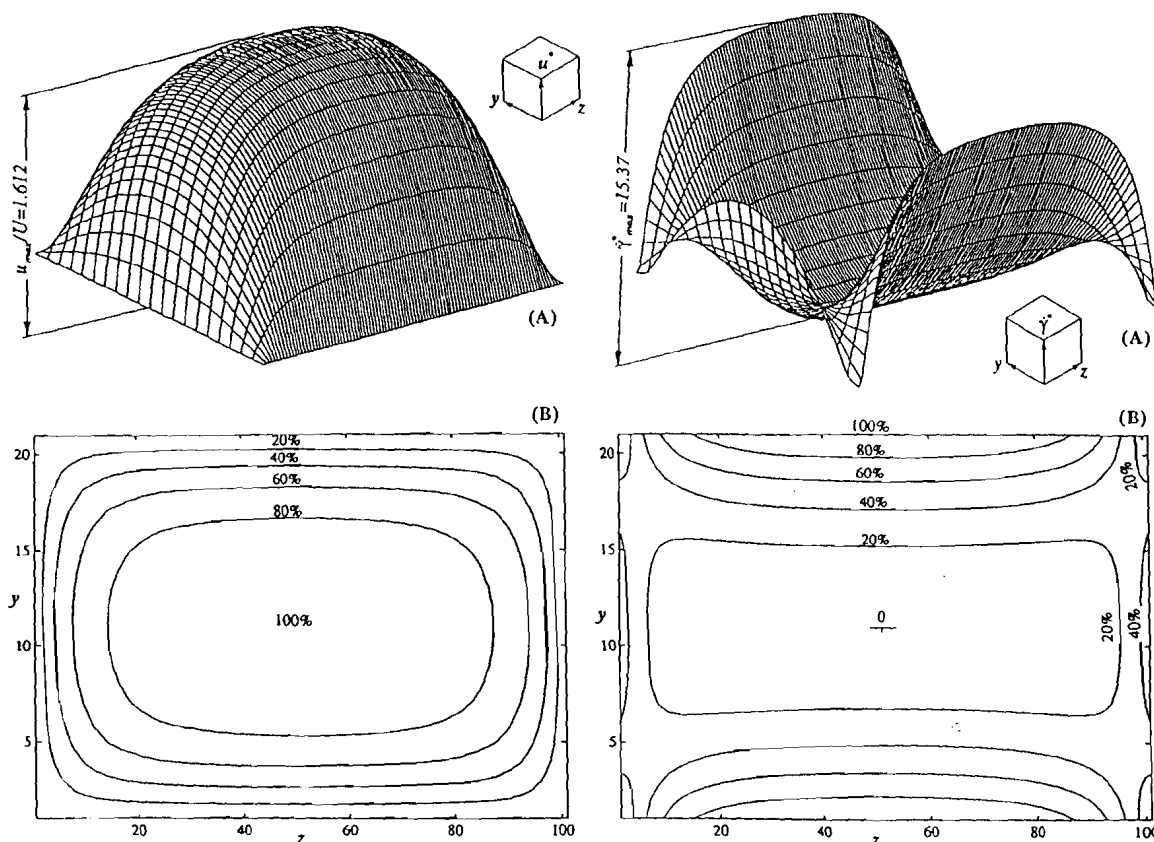


FIG. 6  
(A) Velocity Profile for Real Non-Newtonian Fluid; (B) Corresponding Iso-Velocity Profile

FIG. 7  
(A) Shear Rate Profile for Real Non-Newtonian Fluid; (B) Corresponding Iso-shear-rate Contours

is "thicker," more flat and with smaller center-point velocity than that of FIG.4, which is expected for a pseudoplastic fluid ( $n_{ave}=0.52$ ). Consequently, the shear rates at the walls are higher (compare FIGS.5&7).

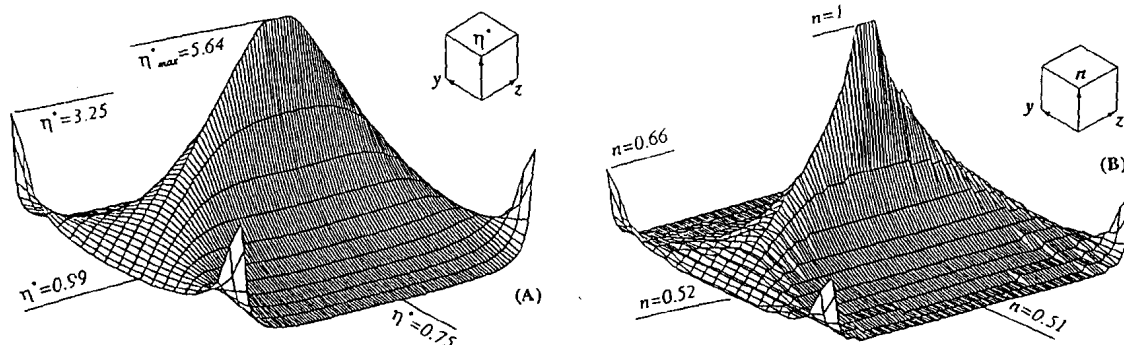


FIG. 8  
(A) Variable Viscosity Profile for Real Non-Newtonian Fluid; (B) Corresponding Variable Power-law Index Profile

TABLE 1  
Maximum, Center-point Dimensionless Velocities

$n \downarrow \alpha^* \rightarrow$	1.00	0.75	0.50	0.25	0.20	0.00
1.50	2.374	2.311	2.243	1.839	1.706	1.60
1.00	2.091	2.071	1.978	1.763	1.706	1.50
<i>real fluid</i>	1.800	1.794	1.766	1.658	1.612	
$n_{avg}=f(\alpha^*)$ $=0.52-0.54$	1.779	1.770	1.745	1.641	1.597	
0.50	1.749	1.744	1.723	1.632	1.589	1.33
0.00	1.000	1.000	1.000	1.000	1.000	1.00

TABLE 2  
Maximum Dimensionless Shear Rates at the Center of Longer Wall

$n \downarrow \alpha^* \rightarrow$	1.00	0.75	0.50	0.25	0.20	0.00
1.50	8.44	8.98	9.31	9.76		10.66
1.00	9.56	10.25	10.76	11.29	11.38	12.00
<i>real fluid</i>	12.44	13.33	14.25	15.30	15.37	
$n_{avg}=f(\alpha^*)$ $=0.52-0.54$	12.34	13.23	14.11	15.26	15.36	
0.50	12.76	13.60	14.45	15.56	15.66	16.00
0.00	$\infty$	$\infty$	$\infty$	$\infty$	$\infty$	$\infty$

TABLE 3  
Dimensionless Shear Rates at the Center of Shorter Wall

$n \downarrow \alpha^* \rightarrow$	1.00	0.75	0.50	0.25	0.20	0.00
1.50	8.44	8.93	7.84	8.00		N/A
1.00	9.56	9.14	8.47	8.31	8.35	N/A
<i>real fluid</i>	12.44	11.37	9.91	8.86	8.69	N/A
$n_{avg}=f(\alpha^*)$ $=0.52-0.54$	12.34	11.35	9.93	8.92	8.76	N/A
0.50	12.75	11.63	10.09	8.96	8.79	N/A
0.00	$\infty$	$\infty$	$\infty$	$\infty$	$\infty$	N/A

TABLE 4  
Dimensionless Shear Rates at the Corner

$n \downarrow \alpha^* \rightarrow$	1.00	0.75	0.50	0.25	0.20	0.00
1.50	1.55	2.44	2.18	2.22		N/A
1.00	0.95	1.73	1.55	1.52	1.52	N/A
<i>real fluid</i>	0.15	0.27	0.63	0.54	0.53	N/A
$n_{avg}=f(\alpha^*)$ $=0.52-0.54$	0.09	0.21	0.51	0.45	0.45	N/A
0.50	0.27	0.34	0.50	0.40	0.39	N/A
0.00	$\infty$	$\infty$	$\infty$	$\infty$	$\infty$	N/A

Another characteristic of a non-Newtonian fluid is variable viscosity across the cross-section (see FIG.8A). Note that the *real* fluid viscosity has a finite value at the center-point as compared to infinite value for the corresponding *average* power-law fluid. For each grid point the actual-measured viscosity function of "*real*" fluid is *locally* represented as simple power-law fluid with appropriate but *varying* power-law and consistency indices, the former being represented on FIG.8B. The values of FIG.8B should be compared to the uniform value of  $n_{av}=0.52$  of the corresponding *average* power-law fluid. Note that on FIGS.4 to 8 the calculated fluid and flow properties are in scale, except for the duct aspect ratio (1:5), due to MATLAB software limitations.

The most characteristic velocity and shear rate results for different ducts and fluids are presented in TABLE 1 and TABLES 2,3,4 respectively, as described in the Result section. The center-point (maximum) velocity increases with an increase of both the aspect ratio and the power-law index. The opposite is true for the maximum shear rate, which occurs at the center of the longer wall.

More complex "*real*" non-Newtonian fluids may be represented with locally varying power-law fluid indices. Such "*real*" fluids may also be represented with the simple "*average*" power-law model by averaging locally varying power-law indices around the perimeter. The velocity, shear-rate and viscosity results of such "*average*" and "*real*" fluids are compared. The agreement is rather good except for the viscosity in a narrow center region due to unreasonably high viscosity prediction of the power-law fluid model for very small shear rates (being infinity for zero shear-rate). However this large viscosity discrepancy in the central region does not affect substantially the shearing stresses due to very small shearing rates in that region. Subsequently, the velocity and shear-rate profiles are shaped by the shearing stresses themselves. Therefore, such a viscosity function simplification has little influence on overall velocity and shear -rate profiles in fully developed non-Newtonian flow in rectangular ducts.

#### Acknowledgement

The author would like to acknowledge that numerical calculations were performed, under his instructions and supervision, by Ms. Jia Wang, the author's ex-graduate student. However, except for one paper [2], she expressed no desire for continuation of this work.

#### Nomenclature

- $a$  longer side of rectangular cross-section, FIG.2
- $a_i$  coefficients in viscosity function, Eq.(3);  $i=0,1,2,3$ .
- $b$  shorter side of rectangular cross-section, FIG.2
- $D_h$  hydraulic diameter [ $D_h=4ab/(a+b)$ ]
- $f$  Fanning friction factor, Eq.(7)

- $K$  consistency index of power-law non-Newtonian fluid, Eq.(2)
- $n$  power-law index of non-Newtonian fluid, Eq.(2)
- $p$  pressure in fluid
- $Re^*$  (generalized) Reynolds number, Eq.(7)
- $u$  fluid velocity component in  $x$  direction
- $U$  average fluid velocity
- $\mathbf{V}$  fluid velocity vector
- $x, y, z$  Cartesian coordinates
- $\alpha^*$  rectangular duct aspect ratio ( $\alpha^* = b/a \leq 1$ )
- $\dot{\gamma}$  shear (strain) rate or shear rate magnitude
- $\eta$  fluid (apparent) viscosity
- $\rho$  fluid density
- $\tau$  shear stress
- $( )_{ref}$  corresponding reference quantity, defined in text between Eq.(6)&(7)
- $( )^*$  dimensionless quantity, ratio between dimensional and corresponding reference quantity

#### References

1. J.P. Hartnett and M. Kostic, "Heat Transfer to Newtonian and Non-Newtonian Fluids in Rectangular Ducts," *Advances in Heat Transfer*, Vol. 19, p. 247-356, Academic Press, (1989).
2. M. Kostic and J. Wang, "Analysis of Newtonian and Non-Newtonian Velocity Profiles in Rectangular Ducts," The 1992 ASME National Fluids Engineering Conference, Los Angeles, California, June 21-24, 1992. *FED-Vol. 133*, p.207, ASME (1992).
3. R.K. Shah and A.L. London, "Laminar Flow Forced Convection in Ducts," *Advances in Heat Transfer*, Supplement 1, Academic Press, (1978).
4. J. Wang, "A Numerical Study of Newtonian and Non-Newtonian Fluids Flow in Rectangular Ducts," *M.S. Thesis*, Northern Illinois University, DeKalb, IL, (1992).
5. S.V. Patankar, *Numerical Heat Transfer and Fluid Flow*, Hemisphere, Washington D.C., (1980).

*Received April 9, 1993*

# INTERNATIONAL COMMUNICATIONS IN HEAT AND MASS TRANSFER A Rapid Communications Journal

## BOARD OF EDITORS

- E. HAHNE**  
Institut für Thermodynamik und Wärmetechnik,  
Pfaffenwaldring 6, D-7000 Stuttgart 80,  
Germany
- J.P. HARTNETT (Coordinating Editor)**  
Energy Resources Center  
University of Illinois, Box 4348  
Chicago, IL 60680 U.S.A.
- P.J. HEGGS**  
Department of Chemical Engineering  
University of Bradford  
Bradford, West Yorkshire BD7 1DP, U.K.
- S.Y. KO (Associate Editor)**  
Institute of Engineering Thermophysics  
Chinese Academy of Sciences  
P.O. Box 2706, Beijing 100080, China
- M. LÉBOUCHE**  
Laboratoire d'Energétique et de Mécanique  
Théorique et Appliquée, CNRS URA 875  
2, Avenue de la Forêt de Haye, BP 160  
54504 Vandoeuvre-lès-Nancy Cedex, France
- O.G. MARTYNYENKO**  
Heat and Mass Transfer Institute  
Byelorussian Academy of Sciences  
25 Podlesnaya, Minsk, Belarus
- W.J. MINKOWYCZ**  
Department of Mechanical Engineering  
University of Illinois, Box 4348  
Chicago, IL 60680 U.S.A.
- B.R. PAI (Associate Editor)**  
National Aeronautical Laboratory  
Post Bag No. 1779  
Bangalore 560017, India
- P.F. PETERSON (Associate Editor)**  
Department of Nuclear Engineering  
University of California  
Berkeley, CA 94720, U.S.A.
- K. SUZUKI (Associate Editor)**  
Department of Mechanical Engineering  
Kyoto University  
Yoshidahonmachi, Kyoto 606, Japan
- I. TANASAWA**  
Institute of Industrial Science  
University of Tokyo  
7-22-1 Roppongi, Minato-ku,  
Tokyo 106, Japan
- C.-L. TIEN**  
University of California  
Berkeley, CA 94720, U.S.A.
- B.X. WANG**  
Thermal Engineering Department  
Tsinghua University, Beijing 100084,  
China

## HONORARY EDITORIAL ADVISORY BOARD

- Co-Chairmen:* **E.R.G. ECKERT**, *University of Minnesota, Minneapolis, MN 55455, U.S.A.*  
**U. GRIGULL**, *Technische Universität, München, Germany*

- J.P. BARDON**, Nantes, France  
**F.J. BAYLEY**, Brighton, U.K.  
**A. BEJAN**, Durham, NC, U.S.A.  
**A.E. BERGLES**, Troy, NY, U.S.A.  
**B.T. CHAO**, Urbana, IL, U.S.A.  
**M. COMBARNOUS**, Talence, France  
**K. CORNWELL**, Edinburgh, U.K.  
**R. COTTA**, Rio de Janeiro, Brazil  
**M. CUMO**, Rome, Italy  
**G. DE VAHL DAVIS**, Kensington,  
Australia  
**A.A. DOLINSKY**, Kiev, Ukraine  
**J.J.D. DOMINGOS**, Lisbon, Portugal  
**R. ECHIGO**, Tokyo, Japan  
**D.K. EDWARDS**, Irvine, CA, U.S.A.  
**Y. FUJITA**, Fukuoka, Japan  
**B. GEBHART**, Philadelphia, PA,  
U.S.A.
- R.J. GOLDSTEIN**, Minneapolis, MN,  
U.S.A.  
**G.F. HEWITT**, London, U.K.  
**C. HOOGENDOORN**, Delft,  
The Netherlands  
**J.R. HOWELL**, Austin, TX, U.S.A.  
**D.B. INGHAM**, Leeds, U.K.  
**T.F. IRVINE, JR.**, Stony Brook, NY,  
U.S.A.  
**S. KAKAC**, Miami, FL, U.S.A.  
**Y. KATTO**, Tokyo, Japan  
**R.T. LAHEY**, Troy, NY, U.S.A.  
**A.I. LEONTIEV**, Moscow, Russia  
**F. MAYINGER**, Munich, Germany  
**M.D. MIKHAILOV**, Sofia, Bulgaria  
**Yu.A. MIKHAILOV**, Riga, Latvia  
**B.B. MIKIC**, Cambridge, MA, U.S.A.  
**Y. MORI**, Tokyo, Japan
- V.E. NAKORYAKOV**, Novosibirsk,  
Russia  
**R.I. NIGMATULIN**, Moscow, Russia  
**F. OGINO**, Kyoto, Japan  
**R. POHORECKI**, Warsaw, Poland  
**G.D. RAITHBY**, Waterloo, Canada  
**U. RENZ**, Aachen, Germany  
**J.F. RICHARDSON**, Swansea, U.K.  
**W. ROETZEL**, Hamburg, Germany  
**J.W. ROSE**, London, U.K.  
**J.-F. SACADURA**, Villeurbanne,  
France  
**VM.K. SASTRI**, Madras, India  
**J. SCHNELLER**, Bechovice,  
Czechoslovakia  
**R.A. SEBAN**, Berkeley, CA, U.S.A.  
**R.K. SHAH**, East Amherst, NY, U.S.A.
- S. SIDEMAN**, Haifa, Israel  
**R. SIEGEL**, Cleveland, OH, U.S.A.  
**H. SIMPSON**, Glasgow, U.K.  
**E.M. SPARROW**, Minneapolis, MN,  
U.S.A.  
**K. STEPHAN**, Stuttgart, Germany  
**M.A. STYRIKOVICH**, Moscow,  
Russia  
**M.G. VELARDE**, Madrid, Spain  
**R. VISKANTA**, West Lafayette, IN,  
U.S.A.  
**D. VORTMEYER**, Munich, Germany  
**D.R. WEBB**, Manchester, U.K.  
**K.T. YANG**, Notre Dame, IN, U.S.A.  
**S.M. YANG**, Shanghai, China  
**A.A. ZHUKAUSKAS**, Vilnius,  
Lithuania

## SUBSCRIPTION INFORMATION

**Production Editor:** Lorraine Petrella, Pergamon Press, Tarrytown, New York.

**Editorial Office:** Professor J.P. Hartnett, Energy Resources Center and Professor W.J. Minkowycz, Department of Mechanical Engineering, The University of Illinois at Chicago, Box 4348, Chicago, IL 60680, USA.

**Publishing, Subscription and Advertising Offices:** Pergamon Press Inc., 660 White Plains Road, Tarrytown, NY 10591-5153, USA, INTERNET "PPI@PERGAMON.COM" and Pergamon Press Ltd., Headington Hill Hall, Oxford OX3 0BW, England.